European Review for Medical and Pharmacological Sciences 2021; 25: 2528-2541

PAX5-induced upregulation of LINC01194 exerts oncogenic properties by regulating GOLPH3 expression *via* miR-486-5p in prostate cancer

H.-R. SONG[1], X.-B. GUO[1], Y. DUAN[1], H.-Y. MENG[2], Z.-Y. WANG[3]

[1]Department of Laboratory Medicine, The First Affiliated Hospital of Zhengzhou University, Zhengzhou, Henan, China
[2]Department of Science and Education, The People's Hospital of Hua Xian, Anyang, Henan, China
[3]Department of Urology, The First Affiliated Hospital of Zhengzhou University, Zhengzhou, Henan, China

Abstract. – OBJECTIVE: Several studies have demonstrated that long non-coding RNA can act as crucial roles during the progression of various tumors, including prostate cancer (PCa). We aimed to determine lncRNA LINC01194(LINC01194) expression in prostate cancer (PCa) and examine its influence on tumor behaviors of PCa cells.

PATIENTS AND METHODS: RT-PCR was performed to examine LINC01194 and PAX5's expression levels in PCa tissues and cell lines. Luciferase reporter and chromatin immunoprecipitation (ChIP) assays were performed to explore whether PAX5 could activate the transcription of LINC01194. Cell viability, migration and invasion were assessed by CCK-8, colony formation, transwell assay and Wound-healing assays. Bioinformatics and Dual-Luciferase assays were used to investigate the interaction between LINC01194 and miR-486-5p, as well as between miR-486-5p and GOLPH3. Western blot was applied for detecting the expressions of the related proteins.

RESULTS: LINC01194 was highly expressed in PCa specimens and cell lines. PAX5 could bind directly to LINC01194 promoter region and activate its transcription. Functionally, the proliferation and metastasis of PCa cells were substantially impeded by LINC01194 silencing in vitro and in vivo. Mechanistically, LINC01194 promoted PCa progression by serving as a sponge of miR-486-5p to increase GOLPH3 expression.

CONCLUSIONS: Our study identifies LINC01194 as a tumor promotor in PCa and implicates the LINC01194/miR-486-5p/GOLPH3 axis in the PCa progression.

Key Words:
LncRNA LINC01194, MiR-486-5p, PAX5, Metastasis, Prostate cancer.

Introduction

Prostate cancer (PCa) is a prevailing malignancy in males worldwide, resulting in an increasing quantity of lethality and morbidity in the last 20 years[1]. The China National Cancer Prevention Center have shown that PCa is sixth in incidence and ninth in mortality[2]. Metastatic PCa could conclusively develop into hormone refractory PCa and androgen independent PCa, which are considered as the leading cause of death in PCa patients[3,4]. Up to date, no effective treatments are available for advanced PCa. Thus, in-depth exploration is required to figure out the potential mechanisms involved in PCa metastasis, which might help identify fresh therapeutic and diagnostic targets.

Long non-coding RNAs (lncRNAs) have a length of over 200 nucleotides[5]. In the past few thirty years, lncRNAs have been judged as the by-products or 'noise' of the transcription of genes[6]. However, growing cellular experiments have caused distinct changes in the function of lncRNAs which may be involved in diverse biological processes, including embryonic developments, cellular growth and tumorigenesis by influencing the expressions of various genes at the transcriptional, post-transcriptional and transcriptional levels[7,8]. LncRNAs played the roles of oncogenes or tumor suppressors in the progression of many types of cancers *via* influencing the apoptosis and metastasis. These findings highlighted the potential of lncRNAs used as novel biological biomarkers and therapeutic targets[9,10]. Although a large number of dysregulated lncRNAs have been identified using

Corresponding Author: Zhi-yong Wang, MD; e-mail: wzy8891001@163.com

microarray analysis, only a small proportion of tumor-specific lncRNAs have been functionally studied.

Herein, LINC01194 as a new PCa-related lncRNA was identified. It was one of the most overexpressed lncRNA according to the data of significance analysis of microarrays. Then, we provided evidence that LINC01194 was distinctly highly expressed in both PCa specimens from 62 PCa patients and cell lines. Previously, the dysregulation of LINC01194 has been demonstrated in colorectal carcinoma and laryngeal squamous cell carcinoma[11,12]. Yet, little knowledge has been obtained regarding its function and expression in other tumors. For the first time, we explored the expression and biological function of LINC01194 in PCa.

Patients and Methods

PCa Patients and Tissue Specimens

The overall 62 normal prostates and paired PCa specimens were provided during 2017-2019 by 62 PCa patients experiencing radical surgery at the First Affiliated Hospital of Zhengzhou University. The inclusion criteria for the patient cohort included (1) having a distinctive pathological diagnosis of PCa; (2) the patients had no previous history of other cancers; and (3) having complete clinicopathological data. An exclusion criterion was that the patients received radiation therapy or chemotherapy before surgery. Written informed consent was obtained from all patients. PCa grading was assessed in accordance with the criteria set by the (International Society of Urological Pathology) 2014 Grading Committee[13,14]. Clinicopathological features of patients are summarized in Table I. The human cancer tissues were used under the approval of the Human Research Ethics Review Board of the First Affiliated Hospital of Zhengzhou University.

Table I. Clinical and pathological parameters of PCa patients.

Characteristics	Group	Total
Age (years)	< 65	27
	≥ 65	35
Tumor size (cm)	< 2.5	32
	≥ 2.5	30
Gleason score	< 7	29
	≥ 7	33
Preoperative PSA level (ng/mL)	< 10	26
	≥ 10	36
Clinical stage	T2	36
	T3-T4	26
Lymph node metastasis	Negative	45
	Positive	17

Bioinformatics Analysis

The StarBase database was applied for the identification of potential miR-lncRNA binding partners[15]. The downstream target genes of these miRs were determined using TargetScan[16]. JASPAR identified the PAX5 binding motif in the promoter region of LINC01194[17].

Cell Culture and Cell Transfections

Non-malignant prostate epithelial cells (RWPE-1) and PCa cells (PC3, DU145 and LNCap) were provided by the American Type Culture Collection (ATCC; Manassas, VA, USA) and cultured in DMEM medium added by 10% FBS (Invitrogen, Haidian, Beijing, China) and streptomycin and penicillin (Invitrogen, Haidian, Beijing, China) at 37°C in a 5% CO_2 humidified atmosphere.

GenePharma (Shanghai, China) was applied to the synthesis of specific short hairpin RNA (sh-LINC01194-2 and sh-LINC01194-1) of LINC01194 and scramble oligonucleotides (sh-NC). A unit of 30 μg of sh-LINC01194-1 and sh-LINC01194-2 or sh-NC was constructed into BLOCK-iT™ lentiviral RNAi expression system (Invitrogen, Haidian, Beijing, China). The synthesis of pcDNA3.1-PAX5 vector(ov-PAX5) and pcDNA3.1-control vector, negative control(-si-NC) and siRNA targeting PAX5(si-PAX5) was performed in Hanheng Company (Pudong, Shanghai, China). Weihui Technology (Changsha, Hunan, China) supplied miR-486-5p mimics, NC mimics, miR-486-5p inhibitors and NC inhibitors. The transfections were carried out applying Lipofectamine 3000 (Invitrogen, Haidian, Beijing, China).

RNA Extraction and Real-Time PCR Analysis

TRIzol reagent (Invitrogen, Carlsbad, CA, USA) was applied to the extraction of total RNA from tissue samples and cells. The PrimeScript RT reagent kit with gDNA Eraser (Takara, Hangzhou, Zhejiang, China) or miRNA cDNA Kit (CWBio, Suzhou, Jiangsu, China) supported the generation of the first-strand cDNA. SYBR® Premix Ex Taq™ II (TaKaRa, Hangzhou, Zhejiang, China) was adopted to carry out qRT-PCR on Applied Biosystems 7500 Real-time PCR System (Applied Biosystems, Foster City, CA,

USA). The reaction conditions were 95°C for 5 min, followed by 40 cycles of 95°C for 15 sec and 60°C for 30 sec. The normalization of LINC01194 and miR-486-5p expressions to U6 or GAPDH was achieved. Table II lists the sequence of used primers. The relative expressions of lncRNAs and mRNA were calculated by the use of the $2^{-\Delta\Delta CT}$ methods. All reactions were repeated three times.

Cell Proliferation Assays

Cell Counting Kit-8 (Solarbio, Tongzhou, Beijing, China) assays were applied for the examination of the proliferation abilities of the cells. DU145 and LNCap cells after transfection for 48 h were seeded into 96-well plates, where the density of each well was 6×10^3 cells. Each well was added with 20 µl of CCK-8 after transcription for 24, 48, 72, and 96 h. An enzyme-labeled analyzer supported the detection of Optical density (OD) when the wavelength was 450 nm.

Colony Formation Assay

For colony formation assays, after transfection of sh-NC, sh-LINC01194-1 or sh-LINC01194-2500, we seeded cells in a six-well plate 48 h and cultured them at 37°C, 5% CO_2 incubator, changing the medium every 2 days. The cell culturing continued for 14 days before cell colonies could be observed. The colonies were immobilized, followed by the dyeing by the use of crystal violet.

5-Ethynyl-2′-Deoxyuridine (EdU) Assays

The EdU Proliferation kit (Abcam, Haidian, Beijing, China) was applied to perform EdU incorporation assays. In brief, sh-NC, sh-LINC01194-2 or sh-LINC01194-1-transfected DU145 and LNCap cells were incubated with 15 µmol/l EdU dye at 37°C for 3 h, and then, fixed and washed by the fixative, stained by Apollo fluorescent dye and HOE-33342(ENZO, Taize Company, Daxing, Beijing, China). Finally, glass slides were used to fix the glass coverslips, followed by the capture by the use of a fluorescent microscopy.

Table II. The primers used in this study for RT-PCR.

Names	Sequences (5′-3′)
LINC01194: F	AGACTGCTCTTGAGGCTGGAGT
LINC01194: R	AGGCTGAGGCTGGAGGATCTCT
PAX5: F	ACTTGCTCATCAAGGTGTCAG
PAX5: R	TCCTCCAATTACCCCAGGCTT
miR-486-5p: F	GTACTGAGCTGCCCCGAGAAA
miR-486-5p: R	CTCGCTTCGGCAGCACA
GOLPH3: F	AGGAAGCCGTTCTTGACAAATG
GOLPH3: R	GGCATGAGCCAGGTAAATGAG
GAPDH: F	CTGGGCTACACTGAGCACC
GAPDH: R	AAGTGGTCGTTGAGGGCAATG
U6: F	GTGCAGGGTCCGAGGT
U6: R	CTCGCTTCGGCAGCACA

Wound-Healing Assays

Transfected DU145 or LNCap cells were seeded into each well of a 6-well plate and incubated overnight to reach near confluence. Using a P200 pipette tip, A linear scratch was made on the monolayer. By the use of PBS, the cells were washed three times, followed by the culture in DMEM medium. Image J software was used to quantify the gaps which were photographed. Each experiment was repeated in triplicates.

Transwell Assays

Transwell assays for the determination of LINC01194 knockdown on the ability of invasion were carried out by the use of transwell plates (Corning, Pudong, Shanghai, China). We plated cells into the upper chamber and filled the lower one with the medium that contained serum. These two were cultured in a 5% CO_2 environment at 37°C for 24 h and 36 h, followed by a 30 min process of fixing with methanol and then a 20 min staining process by Giemsa. Then, a cotton swab was applied to remove cells from the membrane's upper surface. Then, fixing and staining process of 20 min was conducted on the cells that migrated through the membrane to the underside by 0.5% crystal violet. Five fields of each well were randomly gated and counted.

Tumor Xenografts in Nude Mice

Purchased from Huafukang Technology (Haidian, Beijing, China), twelve 6-week 15-22 g male BALB/c mice were kept in a specific pathogen free (SPF) environment for seven days. Either side of the axillary region of male BALB/c nude mice (n=6 per group) was subject to the subcutaneous injection of control sh-NC or sh-LINC01194-1 (4×10^6) stably transfected DU145 cells. Afterward, at an interval of four days, we measured the width and length of the tumor. The formula of length × (width^2/2) was used to obtain the tumor volume after 7 weeks. We sacrificed the mice 28 days after the injection, followed by weighing of the tumors. The animal experimental protocols released by the First Affiliated Hospital of Zhengzhou University were followed in the

whole experiment process under the approval of the Animal Care Committee of the First Affiliated Hospital of Zhengzhou University.

Subcellular Fractionation

Nuclear and cytosolic fraction separation was carried out applying a PARIS™ Kit (AM1921; Invitrogen, Wosheng Technology, Hangzhou, Zhejiang, China), based on the guidelines for the product application. In short, DU145 and LNCap cells (4×10^6 cells) were collected, washed, and placed in 400 µl fractionation buffer. Then, from the nuclear pellets, the cytoplasmic fractions were carefully aspirated away. The nuclear pellets were then lysed using cell disruption buffer. Finally, qPCR assays were performed to determine the collected RNAs.

Chromatin Immunoprecipitation (ChIP) Assays

The Magna ChIP™ Kit (17-10086, MERCK, Yiqi Company, Xuhui, Shanghai, China) was used for ChIP assays. For the produce of DNA-protein cross-links, formaldehyde treatment was conducted on DU145 and LNCap cells. It was followed by the sonication of cell lysates for generating chromatin fragments of 200-300 bp. Then, we immunoprecipitated the lysates and took specific antibodies or IgG as the control. RT-PCR was performed to examine the precipitated chromatin DNA which was recovered.

RNA Pull-Down Assays

The biotinylated RNAs (biotin-NC, biotin-LINC01194) were supplied by Sangon Technology (Pudong, Shanghai, China). Then, lysis buffer containing RNase inhibitors was used to treat DU145 and LNCap cells. Probes were dissolved in wash/binding buffer. streptavidin-coupled magnetic beads were applied to incubate the collected probes for 2 h, followed by the addition of cell lysates for an additional 2 h at 25°C. Finally, the miR-486-5p were purified and its foldchanges were measured using RT-PCR experiments.

Luciferase Reporter Assays

The cloning process into pGL3 plasmid was conducted on the potential miR-486-5p binding sites or mutant of LINC01194 or GOLPH3 3'-UTR and the putative binding sites for PAX5 containing LINC01194 promoter regions. Then, we sequenced the needed clone, named pGL3-LINC01194-wild-type, pGL3-LINC01194-mutant, pGL3-LINC01194-wild-type and pGL3-LINC01194-mutant. Under the support of Lipofectamine 2000, transfection of DU145 and LNCap cells was performed. Before 80% confluence, cells were placed and grew on a 24-well plate. The Luc-Pair™ Duo-Luciferase Assay Kit was used to quantify the Luciferase activity forty-eight hours later.

Western Blot Analysis

DU145 and LNCap cells were collected by the use of protein lysis buffer RIPA (Beyotime, Pudong, Shanghai, China). For the collection of the supernatants, the samples were centrifuged. The samples were centrifuged for supernatant collection. The BCA Protein Assay kit based on the manufacturer's guidelines (Jinfusai Technology, Haidian, Beijing, China) was applied to obtaining protein concentrations. After the separation process using 10% sodium dodecyl sulfate-polyacrylamide gel electrophoresis, we placed equal amounts of protein (20 µg) onto polyvinylidene difluoride membranes (Millipore, Suzhou, Jiangsu, China) blocked with 5% skim milk at room temperature for 1 h. Afterward, we applied primary antibodies (1:1,000), including anti-GAPDH, anti-GOLPH3, anti-Vimentin, anti-PAX5, anti-N-cadherin, and anti-E-cadherin (Santa Cruz Biotechnology, Haidian, Beijing, China), for incubation overnight at 4°C. After one hour of washing with TNT buffer (abs42156919, Absin, AIbixin, Pudong, China), the membranes were incubated with HRP-conjugated anti-rabbit IgG (1:20,000) antibodies for 1 hour at 25°C. Subsequently, the above membranes were subject to further washing with TNT buffer (abs42156919, Absin, AIbixin, Pudong, China). The visualization of bands was achieved with the Western Lightning Plus-ECL kit.

Statistical Analysis

All statistical analyses were performed using the SPSS v16.0 statistical software package (SPSS, Inc., Chicago, IL, USA). The Student's *t*-test was used to compare the differences between two groups. One-way ANOVA and Tukey post-hoc tests were performed to analyze the difference among three or above groups. This study adopted ROC curve for analyzing the efficacy of LINC01194 in the diagnosis of PCa specimens from non-tumor specimens. A $p < 0.05$ was considered statistically significant. Data were presented as mean ± standard error of the mean from at least three independent experiments.

Results

Upregulation of LINC01194 Expression in PCa

In order to screen functional lncRNAs in PCa, we performed ChIP-seq data using 5 pairs of PCa specimens and matched non-tumor specimens. As shown in Figure 1A, the top 100 dysregulated lncRNAs were shown in Heat Map and Clustering Analysis. LINC01194 was observed to be one of the most upregulated lncRNA in PCa (Figure 1B). Compared with matched non-tumor specimens, PCa specimens displayed an evident increase in LINC01194 expression as revealed by the results of RT-PCR (Figure 1C). Moreover, an increased level of LINC01194 was also shown in three PCa cells compared with RWPE-1 cells (Figure 1D). We further explored whether LINC01194 could have a diagnostic value. An AUC value of 0.7901 (95% CI: 0.7104 to 0.8697) for PCa was obtained by LINC01194 expression in ROC assays (Figure 1E). Our findings suggested LINC01194 as a functional modulator in PCa progression.

PAX5 Activates LINC01194 Transcription in PCa Cells

SP1, STAT3, and other transcription factors have been confirmed to be able to activate the transcription of downstream targets like lncRNAs[18,19]. The use of the JASPAR online database presented the possible binding of PAX5 to the high-score LINC01194 promoter region (Figure 2A and 2B). By analyzing TCGA datasets, significantly higher PAX5 expression in PCa specimens than in non-tumor specimens was found (Figure 2C). In our cohort, we also observed an upregulated expression of PAX5 in PCa specimens (Figure 2D). Moreover, ROC assays confirmed the diagnostic value of high

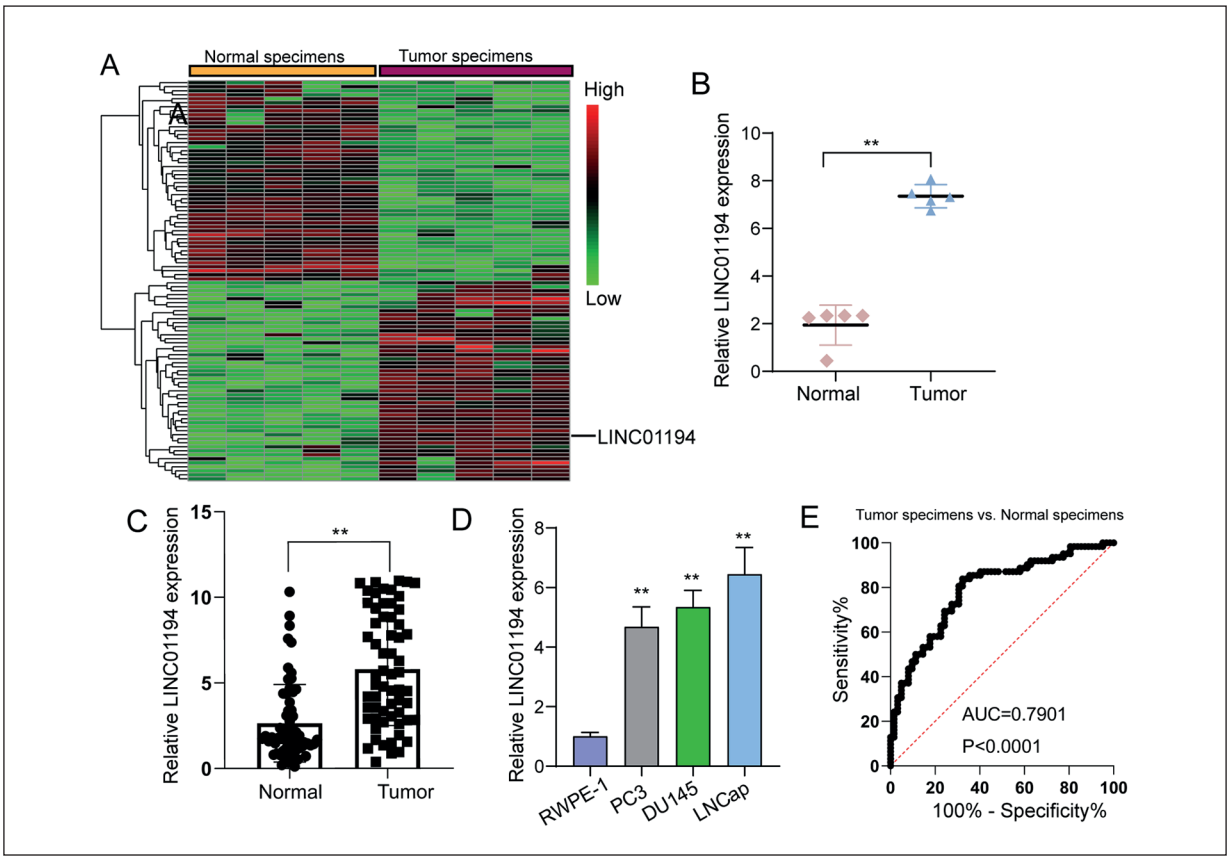

Figure 1. LINC01194 is overexpressed in PCa specimens and cell lines. **A,** Heat map analysis of the lncRNAs expression of groups was created using a method of hierarchical clustering. **B,** The levels of LINC01194 in 5 pairs of PCa specimens and non-tumor tissues. **C,** Relative expression of LINC01194 in PCa tissues and adjacent healthy tissues from 62 patients using RT-PCR. **D,** The expressions of LINC01194 were measured by RT-PCR in the RWPE-1 and various PCa cell lines (PC3, DU145 and LNCap). **E,** ROC assays showed the diagnostic value of LINC01194 in distinguishing PCa specimens from non-tumor specimens. $^{**}p<0.01$.

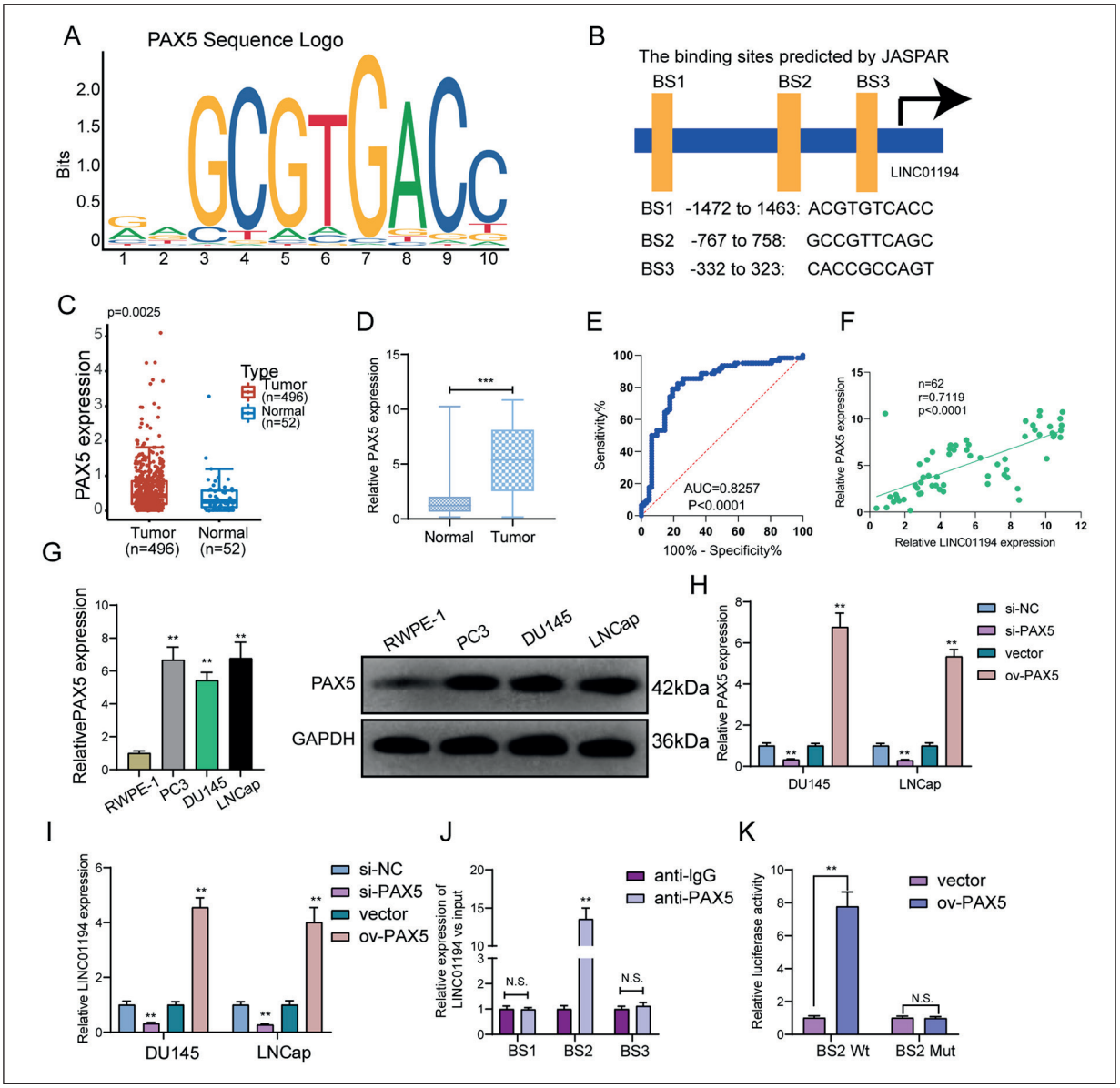

Figure 2. LINC01194 is activated by PAX5 in PCa. **A, B,** PAX5 binding site prediction in the LINC01194 promoter region using JASPAR. **C,** The expression of PAX5 in 496 PCa specimens and 52 non-tumor tissues from TCGA datasets. **D,** RT-PCR examined the levels of LINC01194 in 62 pairs of PCa specimens and non-tumor tissues. **E,** The diagnostic value of LINC01194 expression for PCa specimens in our cohort. **F,** The correlation between LINC01194 and PAX5 expression analyzed in 62 paired PCa samples. **G,** The expression of PAX5 at both mRNA and protein levels was distinctly upregulated in three PCa cells compared to RWPE-1 cells. **H,** The dysregulation of PAX5 expression in DU145 and LNCap cells after overexpression or knockdown of PAX5. **I,** The dysregulation of LINC01194 expression in DU145 and LNCap cells after overexpression or knockdown of PAX5. **J,** ChIP-qPCR analysis of PAX5 occupancy in the LINC01194 promoter in DU145 cells. **K,** Luciferase reporter assay was applied to verify the targeted binding effect between LINC01194 and PAX5 in DU145 cells. $^{**}p<0.01$, $^{***}p<0.01$.

PAX5 expression for PCa specimens with an AUC=0.8275 (Figure 2E). A positive correlation of PAX5 expression with LINC01194 in 62 PCa tissues was revealed by correlation analysis ($p < 0.0001$; Figure 2F). Moreover, the expression of PAX5 at both mRNA and protein levels was distinctly upregulated in three PCa cells compare to RWPE-1 cells (Figure 2G). In addition, after knockdown of PAX5, LINC01194 expression was distinctly decreased in DU145 and LNCap cells, while the overexpression of PAX5 resulted in a distinct regulation of LINC01194 expression in DU145 and LNCap cells (Figure 2H and 2I). Next, ChIP assays indicated that PAX5 might

bind with the BS2 site of LINC01194 promoter (Figure 2J). Subsequently, Luciferase activity assays suggested that increasing PAX5 expression by transfecting pcDNA3.1-PAX5 could markedly accelerate Luciferase activity in DU145 cells transfected with BS2 wild-type (BS2 wt) reporters, while there were no influences on Luciferase activities in DU145 cells when they were co-treated with pcDNA3.1-PAX5 vectors and BS2 mutated-type (BS2 mut) reporters (Figure 2K).

Knockdown of LINC01194 Suppresses Cell Viability and Metastasis of DU145 and LNCap Cells

For an investigation of LINC01194's biological function in PCa cell subtypes, shRNAs were used to suppress LINC01194 expression. As revealed by RT-PCR, LINC01194 expression was distinctly suppressed in DU145 and LNCap cells transfected with sh-LINC01194-1 or sh-LINC01194-2 compared to sh-NC group (Figure 3A). CCK-8 assays revealed that downregulation of LINC01194 remarkably inhibited the growth of cells over time (Figure 3B). Colony formation assays showed cell transfected with sh-LINC01194-1 or sh-LINC01194-2 formed distinctly less colonies than those transfected with sh-NC (Figure 3C). Moreover, an evident reduction in the EdU-positive rate of DU145 and LNCap cells by knockdown of LINC01194 was displayed by EdU proliferation assays (Figure 3D). Also, the exploration of the tumor-suppressing effects of sh-LINC01194-1 *in vivo* based on the Xenografts model indicated the slower tumor growth speed on nude mice and the lower tumor volume and weight of the sh-LINC01194-1 group than those of the sh-NC group (Figures 3E-3G). We also used Wound Healing assays and transwell assays to explore how LINC01194 affected the migration and invasion ability of DU145 and LNCap cells. We observed that knockdown of LINC01194 distinctly reduced the migration distance in DU145 and LNCap cells (Figure 4A). As found from the transwell assays, the invasive capacity of the cells was significantly decreased by LINC01194 knockdown (Figure 4B). Moreover, we examined the influence of LINC01194 knockdown on the EMT progress, finding that the downregulation of LINC01194 suppressed the expression of N-cadherin and Vimentin cells, while promoted the expression of E-cadherin (Figure 4C). Overall, our findings suggested LINC01194 as an oncogenic lncRNA in PCa progression.

LINC01194 Acts as a Molecular Sponge for MiR-486-5p in PCa cells

Then, how LINC01194 contributed to the malignant phenotypes of PCa cells was investigated. The subcellular fractionation revealed LINC01194 expression both in the nucleus and cytoplasm, more in the cytoplasm (Figure 5A). As found by StarBase 3.0, miR-486-5p is a possible potential target of LINC01194 (Figure 5B). By analyzing TCGA datasets, miR-486-5p expression was found to distinctly decreased in PCa specimens (Figure 5C). A similar expressing trend was also observed in our cohort using RT-PCR (Figure 5D). In addition, in three PCa cells, miR-486-5p was found to display a lower level (Figure 5E). Moreover, we performed transwell assays, finding that the invasion of DU145 and LNCap cells (Figure 5F) was highly hindered by miR-486-5p overexpression. Previously, several studies[20,21] have reported the overexpression of miR-486-5p and its anti-oncogenic roles in several types of tumors, including PCa, which was consistent with our findings. Then, miR-486-5p was confirmed by the results of RNA-pull down to combine LINC01194 (Figure 5G). More importantly, the results of Dual-Luciferase reporter assays revealed the decreased Luciferase activity of the Luciferase reporter containing LINC01194-Wt by miR-486-5p overexpression. Nevertheless, these results were not observed in LINC01194-Mut (Figure 5H). In addition, LINC01194 knockdown distinctly suppressed the expression of miR-486-5p, and the downregulation of LINC01194 expression was caused by miR-486-5p overexpression (Figure 5I and 5J). Our findings suggested LINC01194 may competitively sponge miR-486-5p.

LINC01194 Promotes PCa Progression Via sponging miR-486-5p/GOLPH3

For screening miR-486-5p targets, we firstly conducted the analysis of GSE3868 containing 22 PCa specimens and 8 non-tumor prostate specimens using "R". The total 256 dysregulated genes were shown using Heat Map and Volcano plot (fold change [FC] > 5 and adjusted *p*-value [p-adj] < 0.05) (Figure 6A and 6B). Importantly, GOLPH3 was one of the most upregulated genes in PCa specimens (Figure 6C). In addition, we analyzed the TCGA data, finding that GOLPH3 was also highly expressed in PCa. ROC assays also confirmed its diagnostic value in screening PCa specimens from normal tissues (Figure 6E). The above results confirmed that GOLPH3 was

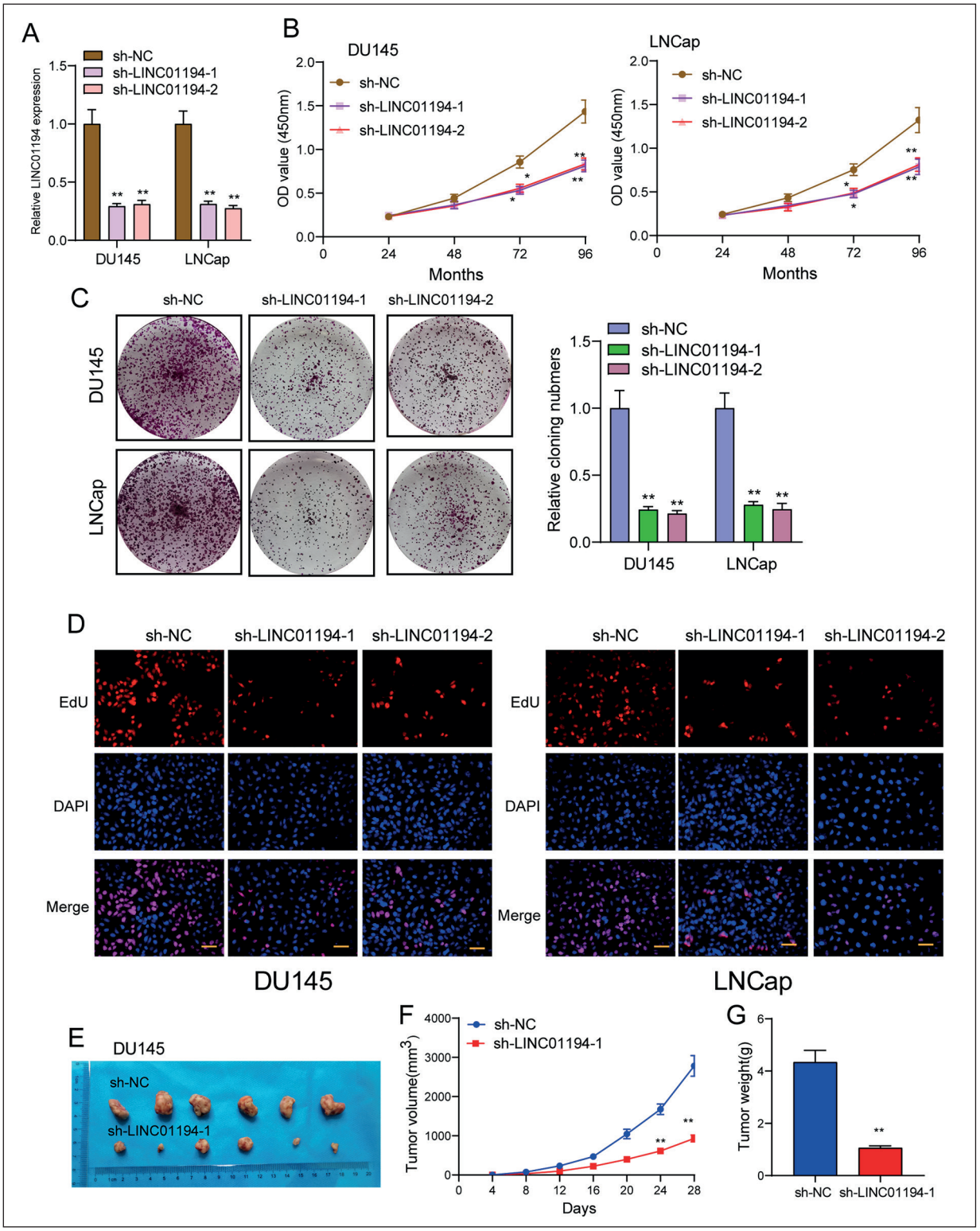

Figure 3. Knockdown of LINC01194 suppressed cell proliferation of glioma cells. **A,** Knocking down of LINC01194 in DU145 and LNCap cells by using sh-LINC01194-1 and sh-LINC01194-2. Statistical analysis was performed by one-way ANOVA with Tukey's post-hoc test. **B,** Quantitative analysis of cell viability detected by CCK-8 assays. **C,** Colony formation assays were performed on DU145 and LNCap cells after knockdown of LINC01194 for 2 weeks. **D,** EdU were performed to detect cell proliferation (magnification: 100×). **E,** Tumors derived from mice in two different groups were presented. **F, G,** Volume and weight of tumors obtained from two groups were measured and shown. $^{**}p<0.01$.

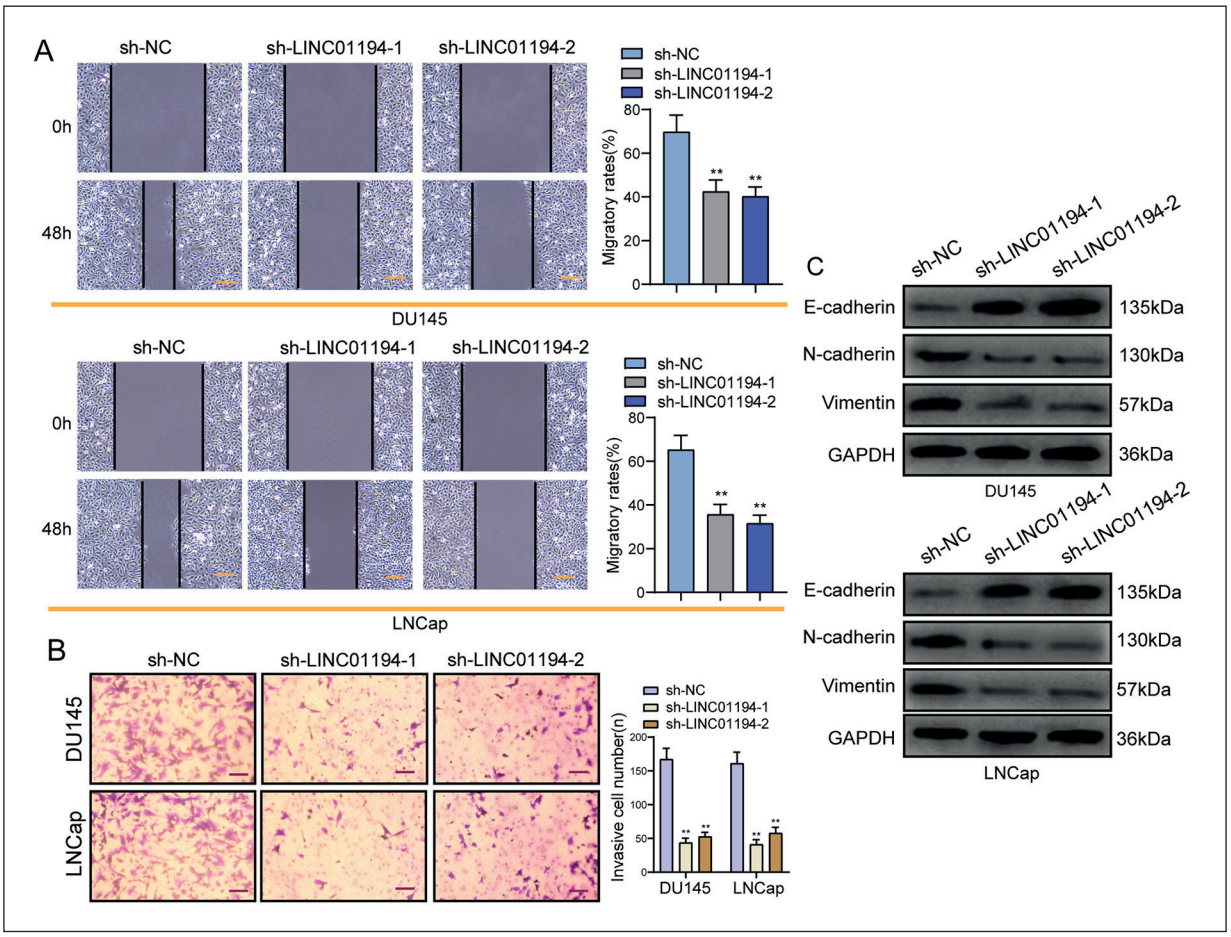

Figure 4. LINC01194 promoted invasion and migration in PCa. **A, B,** The effects of LINC01194 knockdown on the migration (**A**) and invasion (**B**) of DU145 and LNCap cells were examined by wound-healing assays or transwell Assays, respectively (magnification: 40×). **C,** Western blot was utilized to measure the protein levels of epithelial markers (E-cadherin) and mesenchymal markers (Vimentin and N-cadherin) after LINC01194 downregulation in DU145 and LNCap cells. $^{**}p<0.01$.

a tumor promotor in PCa. Previously, GOLPH3's role in promoting the proliferation and metastasis of PCa cells was reported, which demonstrated our findings[22,23]. Interestingly, by the use of StarBase 3.0, we found that GOLPH3 may be a target of miR-486-5p (Figure 6F). RT-PCR further confirmed GOLPH3 was overexpressed in three PCa cells (Figure 6G). As revealed from the outcomes of the Luciferase reporter test, the upregulation of miR-486-5p could decrease GOLPH3-WT activity, but it had no effect on GOLPH3-MUT in both DU145 and LNCap cells (Figure 6H). Also, the expression of GOLPH3 was hindered by miR-486-5p overexpression at both mRNA and protein levels (Figure 6I). Our findings suggested GOLPH3 may be a target of miR-486-5p. Rescue experiments were carried out to further explore whether miR-486-5p and GOLPH3 are responsible for LINC01194-mediated effects on PCa cells. LINC01194 knockdown in DU145 and LNCap cells caused upregulation of GOLPH3 expression, which was found reversed by the downregulation of miR-486-5p (Figure 7A). In addition, as found in functional assays, miR-486-5p exhaustion in DU145 and LNCap cells weakened the role of silencing LINC01194 in suppressing the proliferation and invasion (Figure 7B-7D). Collectively, LINC01194 may serve as a tumor promotor in PCa through the regulation of the miR-486-5p/GOLPH3 axis.

Discussion

Growing studies[24,25] have suggested the possibly important role of lncRNAs in tumorigenesis

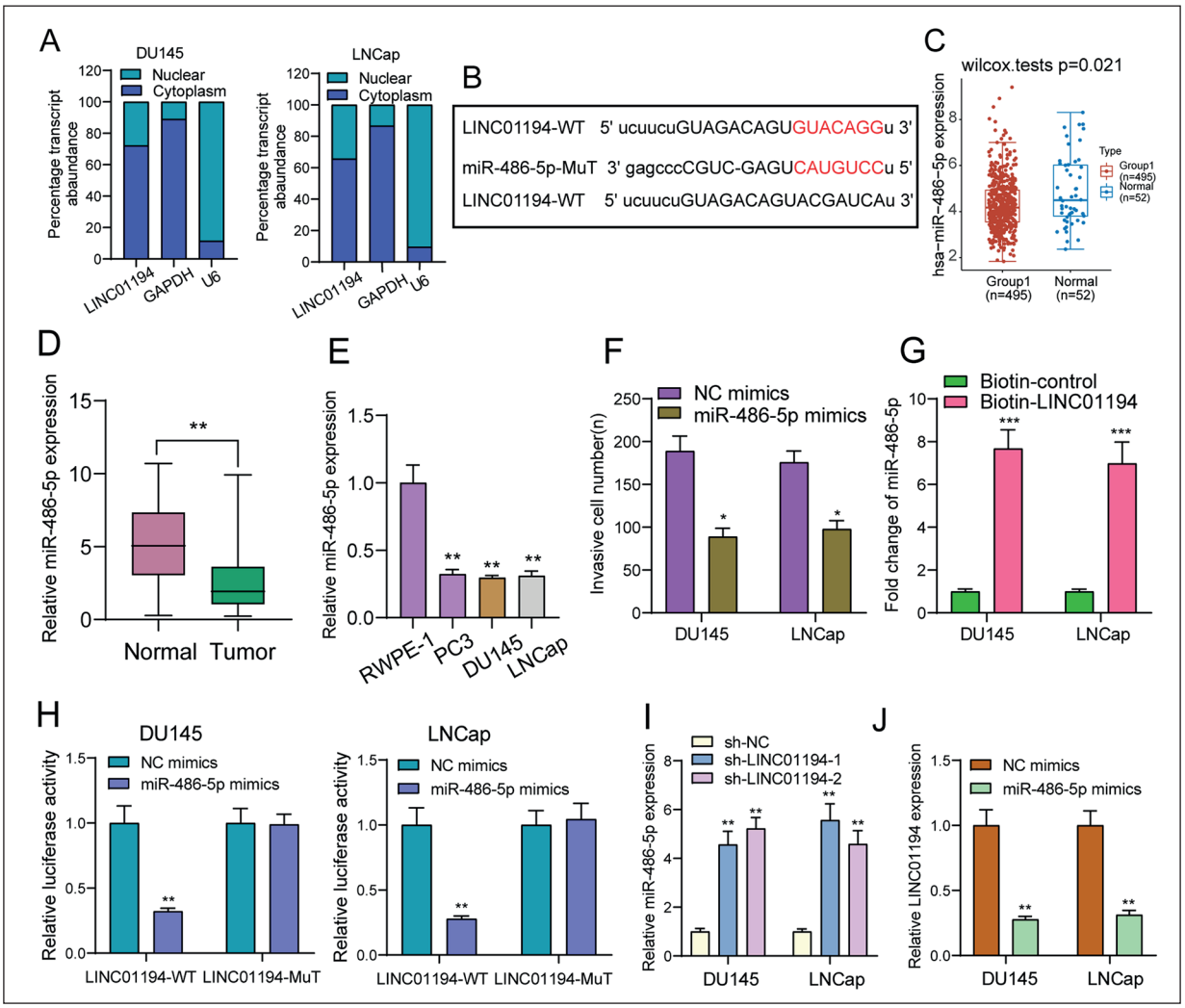

Figure 5. LINC01194 functions as a miR-486-5p sponge in PCa cells. **A,** Relative LINC01194 expression levels in nuclear and cytosolic fractions of DU145 and LNCap cells. **B,** Diagram of the miR-486-5p putative binding sites and corresponding mutant sites in LINC01194 mRNA sequences. **C,** The expression of miR-486-5p in 495 PCa specimens and non-tumor specimens by amazing TCGA datasets. **D,** RT-PCR for the expression of miR-486-5p in our cohort. **E,** MiR-486-5p levels in different PCa cell lines were measured by RT-PCR. **F,** Invasion ability was explored in DU145 and LNCap cells transfected with NC mimics or miR-486-5p mimics, using transwell invasion assays. **G,** RNA pull-down verifying LINC01194 binding to miR-486-5p. **H,** Luciferase reporter assays were conducted to confirm the direct binding between miR-486-5p and LINC01194 in DU145 and LNCap cells. **I,** The expression of miR-486-5p in DU145 and LNCap cells transfected with sh-LINC01194-1, sh-LINC01194-2 or sh-NC. **J,** Overexpression of miR-486-5p resulted in the downregulation of LINC01194. $^{**}p < 0.01$. $^{*}p < 0.05$.

and served as tumor promotors or anti-oncogenes based on the types of tumors. Up to date, several lncRNAs have been identified the dysregulated lncRNAs in PCa, and their tumor-related functions were also functionally elucidated[26,27]. One of these is lncRNA PCAT-1 which was a highly expressed lncRNA and served as a tumor promotor affecting PCa metastasis[28]. Here, this paper presented an increasing LINC01194 expression in PCa, which has a high diagnostic value in screening PCa specimens from non-tumor tissues, indicating it as a novel diagnostic biomarker for PCa patients.

Recently, Long et al[29] revealed that transcription factors may regulate lncRNAs expression, just like some protein-coding genes. For instance, lncRNA HOXD-AS1 transcription was activated by STAT3 in liver cancer[30]. Our study proved PAX5's role in activating LINC01194 upregulation in PCa. Previously, the knockdown of

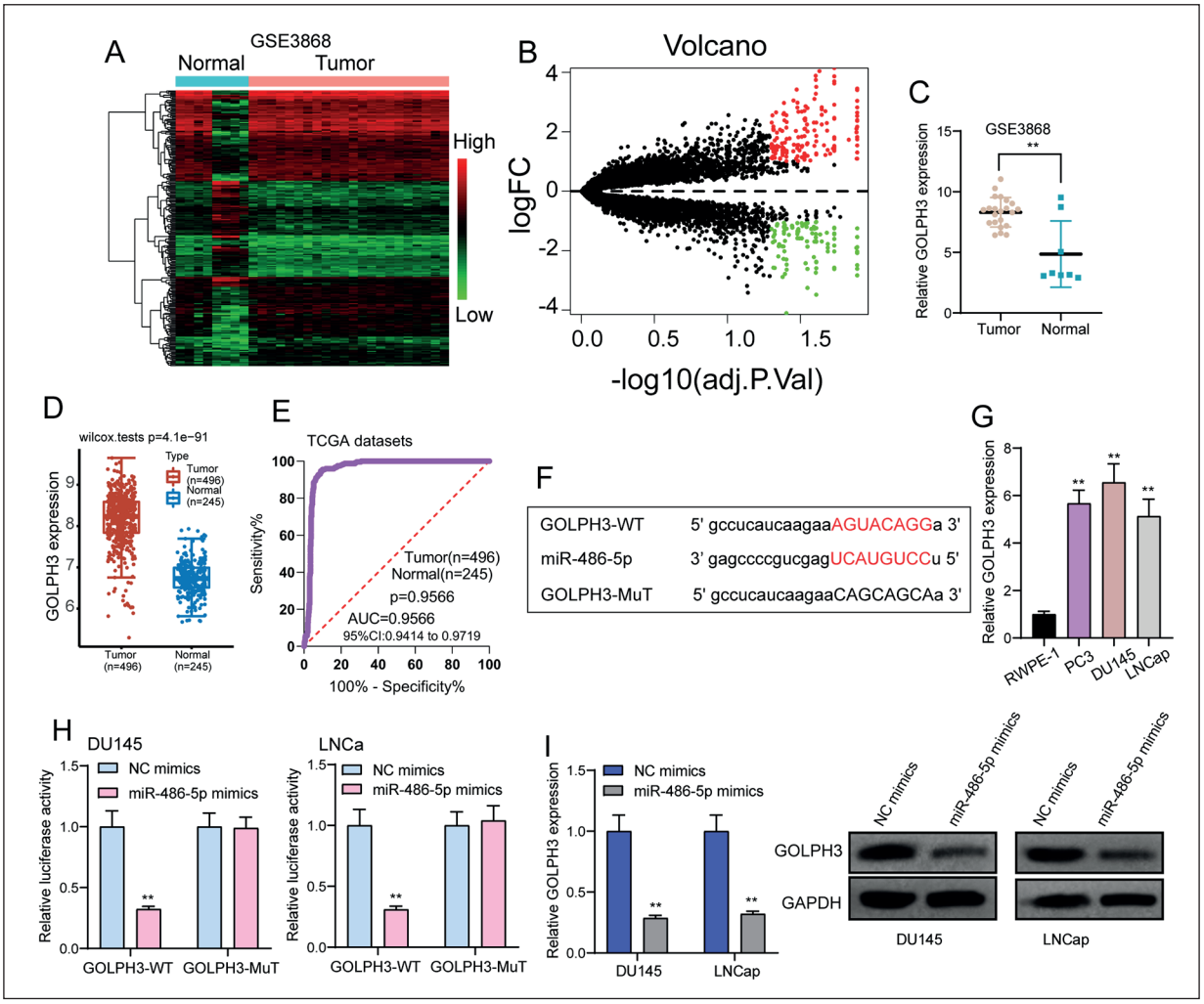

Figure 6. MiR-486-5p targeted GOLPH3 directly. **A,** The dysregulated 286 genes were shown in Heat Map based on GSE3868. **B,** Volcano plot of dysregulated genes. **C,** GOLPH3 expression levels in PCa tissues compared with normal tissues in GSE3868 datasets. **D,** GOLPH3 was overexpressed in PCa specimens in TCGA datasets. **E,** ROC showed the diagnostic value of GOLPH3 expression for PC specimens. **F,** Putative binding site between miR-486-5p and GOLPH3 through TargetScan online software. **G,** The levels of GOLPH3 in three PCa cells and RWPE-1 cells by RT-PCR. **H,** Luciferase reporter assay for analysis of the interaction between miR-486-5p and GOLPH3. **I,** Overexpression of miR-486-5p suppressed the expression of GOLPH3 at both mRNA and protein levels. $^{**}p<0.01$.

PAX5 reportedly suppressed the tumor progression in tumors of several types[31]. In addition, lncRNA FOXP4-AS1 was shown to be activated by PAX5 and exhibit a high level in PCa cells[32]. These findings revealed that PAX5 may activate multiple targets. Then, as found *in vitro* and *in vivo* assays, the proliferation, migration, invasion and EMT progress of PCa cells were found to be hindered by LINC01194 knockdown. As the main progress involved in tumor-to-tumor metastasis, EMT leads to cell-cell adhesion loss and strengthens the abilities of invasion and migration. Our findings revealed the possible contribution of the LINC01194/EMT axis to PCa metastatic properties. In addition, in colorectal carcinoma and laryngeal squamous cell carcinoma, the oncogenic effects of LINC01194 were also confirmed using a series of functional experiments.

After confirming the oncogenic roles of LINC01194 in PCa, our group examined the molecular mechanisms responsible for the altered malignant phenotypes. It has been indicated that mRNA stability and protein localization can be modulated by cytosolic lncRNAs as microRNA sponge[33]. LINC01194 expression was mainly found in the cytoplasm. The results of bioinformatic assays, RNA-pull down assays

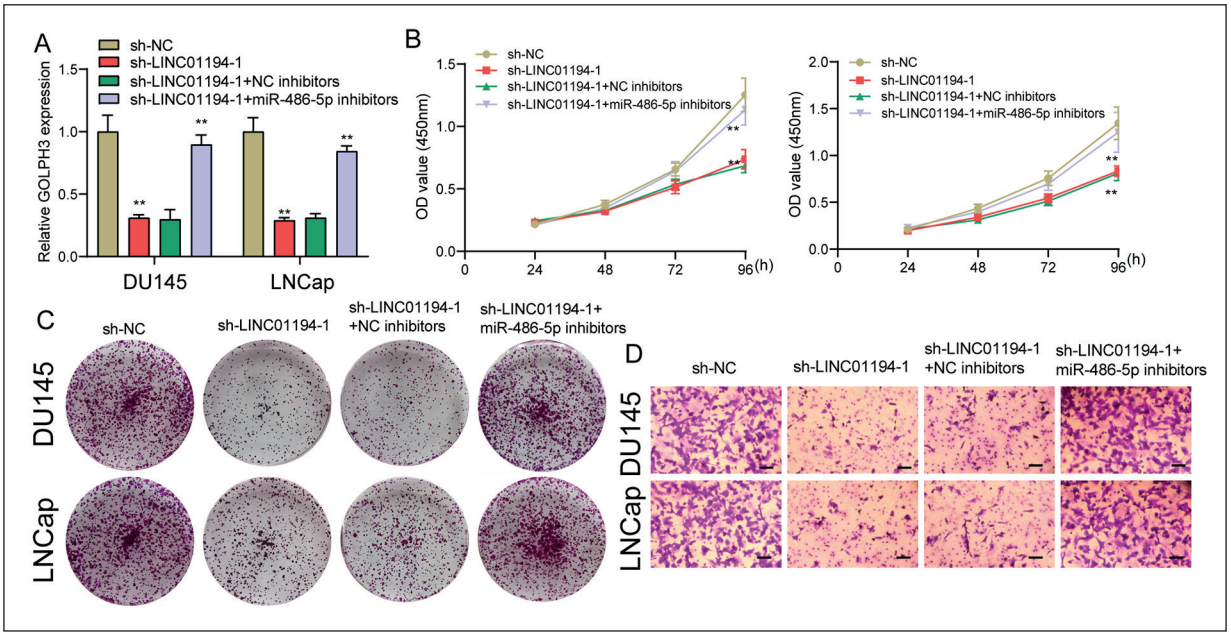

Figure 7. LINC01194 promoted PCa progression by regulating miR-486-5p/GOLPH3 axis. **A,** RT-PCR for the expression of GOLPH3 in DU145 cells and LNCap cells transfected with sh-NC, sh-LINC01194-1, sh-LINC01194-1+NC inhibitors or sh-LINC01194-1+miR-486-5p inhibitors. The CCK-8 assays (**B**), colony formation assays (**C**) and Cell invasion (**D**) assays following knockdown of LINC01194 and/or inhibition of miR-486-5p. (magnification: 40×). *p<0.05, **p<0.01. **p<0.01.

and Luciferase reporter assays demonstrated LINC01194's direct interaction with miR-486-5p. In the literature, the role of miR-486-5p in the progression of several tumors was reported. In PCa, high expression of miR-486-5p was found and its knockdown hindered the proliferation and metastasis of PCa cells *via* targeting Snail[21]. We found that the suppression of LINC01194 was caused by miR-486-5p overexpression, suggesting that LINC01194 may advance PCa cells' proliferation and metastasis *via* sponging miR-486-5p.

Golgi phosphoprotein 3 (GOLPH3), located on 5p13.3, is a highly conserved protein across eukaryotic kingdom and has been confirmed to be involved in protein trafficking, glycosylation and DNA damage-induced Golgi dispersal[34]. Recently, several studies[35-37] demonstrated that GOLPH3 was implicated in tumor growth and metastasis in several types of tumors, such as glioma, epithelial ovarian cancer and bladder cancer. In PCa, increased expression of GOLPH3 and its oncogenic roles were also reported in several studies[22,23]. This study revealed the ability of miR-486-5p to directly target GOLPH3 3'UTR and regulating its expression. Additionally, miR-486-5p overexpression caused a significant reduction in GOLPH3 expression. Moreover, we explored whether there is a ceRNA regulatory axis among LINC01194, miR-486-5p, and GOLPH3 in PCa cells. According to the results of rescue assays, downregulation of miR-486-5p reversed the influence of LINC01194 knockdown on PCa cell proliferation, migration and invasion. These demonstrations partly explained the mechanism by which LINC01194/miR-486-5p participated in PCa progression.

Conclusions

Our study first revealed that LINC01194 expression was an overexpressed lncRNA in PCa and its high expression was induced by PAX5. LINC01194 served as a tumor promotor through the regulation of the miR-486-5p/GOLPH3 axis. However, the underlying mechanism by which LINC01194 could influence other tumor-related genes or regulatory network requires further studies. LINC01194 is a potential target for the diagnosis and treatment of PC in the future.

Conflict of Interest

The Authors declare that they have no conflict of interests.

References

1) de Martel C, Georges D, Bray F, Ferlay J, Clifford GM. Global burden of cancer attributable to infections in 2018: a worldwide incidence analysis. Lancet Glob Health 2020; 8: e180-e190.
2) Chen W, Zheng R, Baade PD, Zhang S, Zeng H, Bray F, Jemal A, Yu XQ, He J. Cancer statistics in China, 2015. CA Cancer J Clin 2016; 66: 115-132.
3) Teo MY, Rathkopf DE, Kantoff P. Treatment of advanced prostate cancer. Annu Rev Med 2019; 70: 479-499.
4) Gamat M, McNeel DG. Androgen deprivation and immunotherapy for the treatment of prostate cancer. Endocr Relat Cancer 2017; 24: T297-t310.
5) Jarroux J, Morillon A, Pinskaya M. History, discovery, and classification of lncRNAs. Adv Exp Med Biol 2017; 1008: 1-46.
6) Jathar S, Kumar V, Srivastava J, Tripathi V. Technological developments in lncRNA biology. Adv Exp Med Biol 2017; 1008: 283-323.
7) Gloss BS, Dinger ME. The specificity of long noncoding RNA expression. Biochim Biophys Acta 2016; 1859: 16-22.
8) Ferrè F, Colantoni A, Helmer-Citterich M. Revealing protein-lncRNA interaction. Brief Bioinform 2016; 17: 106-116.
9) Huarte M. The emerging role of lncRNAs in cancer. Nat Med 2015; 21: 1253-1261.
10) Kondo Y, Shinjo K, Katsushima K. Long non-coding RNAs as an epigenetic regulator in human cancers. Cancer Sci 2017; 108: 1927-1933.
11) Liu DM, Yang H, Yuan ZN, Yang XG, Pei R, He HJ. Long noncoding RNA LINC01194 enhances the malignancy of laryngeal squamous cell carcinoma by sponging miR-655 to increase SOX18 expression. Biochem Biophys Res Commun 2020; 529: 148-155.
12) Wang X, Liu Z, Tong H, Peng H, Xian Z, Li L, Hu B, Xie S. Linc01194 acts as an oncogene in colorectal carcinoma and is associated with poor survival outcome. Cancer Manag Res 2019; 11: 2349-2362.
13) Gordetsky J, Epstein J. Grading of prostatic adenocarcinoma: current state and prognostic implications. Diagn Pathol 2016; 11: 25.
14) Epstein JI, Egevad L, Amin MB, Delahunt B, Srigley JR, Humphrey PA. The 2014 International Society of Urological Pathology (ISUP) Consensus Conference on Gleason Grading of Prostatic Carcinoma: definition of grading patterns and proposal for a new grading system. Am J Surg Pathol 2016; 40: 244-252.
15) Li JH, Liu S, Zhou H, Qu LH, Yang JH. StarBase v2.0: decoding miRNA-ceRNA, miRNA-ncRNA and protein-RNA interaction networks from large-scale CLIP-Seq data. Nucleic Acids Res 2014; 42: D92-97.
16) Agarwal V, Bell GW, Nam JW, Bartel DP. Predicting effective microRNA target sites in mammalian mRNAs. eLife 2015; 4: e05005
17) Khan A, Fornes O, Stigliani A, Gheorghe M, Castro-Mondragon JA, van der Lee R, Bessy A, Chèneby J, Kulkarni SR, Tan G, Baranasic D, Arenillas DJ, Sandelin A, Vandepoele K, Lenhard B, Ballester B, Wasserman WW, Parcy F, Mathelier A. JASPAR 2018: update of the open-access database of transcription factor binding profiles and its web framework. Nucleic Acids Res 2018; 46: D260-d266.
18) Wang ZY, Duan Y, Wang P. SP1-mediated upregulation of lncRNA SNHG4 functions as a ceRNA for miR-377 to facilitate prostate cancer progression through regulation of ZIC5. J Cell Physiol 2020; 235: 3916-3927.
19) Chen JF, Wu P, Xia R, Yang J, Huo XY, Gu DY, Tang CJ, De W, Yang F. STAT3-induced lncRNA HAGLROS overexpression contributes to the malignant progression of gastric cancer cells via mTOR signal-mediated inhibition of autophagy. Mol Cancer 2018; 17: 6.
20) Liu C, Li M, Hu Y, Shi N, Yu H, Liu H, Lian H. MiR-486-5p attenuates tumor growth and lymphangiogenesis by targeting neuropilin-2 in colorectal carcinoma. Onco Targets Ther 2016; 9: 2865-2871.
21) Zhang X, Zhang T, Yang K, Zhang M, Wang K. MiR-486-5p suppresses prostate cancer metastasis by targeting Snail and regulating epithelial-mesenchymal transition. Onco Targets Ther 2016; 9: 6909-6914.
22) Hua X, Xiao Y, Pan W, Li M, Huang X, Liao Z, Xian Q, Yu L. MiR-186 inhibits cell proliferation of prostate cancer by targeting GOLPH3. Am J Cancer Res 2016; 6: 1650-1660.
23) Li W, Guo F, Gu M, Wang G, He X, Zhou J, Peng Y, Wang Z, Wang X. Increased expression of GOLPH3 is associated with the proliferation of prostate cancer. J Cancer 2015; 6: 420-429.
24) Peng WX, Koirala P, Mo YY. LncRNA-mediated regulation of cell signaling in cancer. Oncogene 2017; 36: 5661-5667.
25) Li J, Meng H, Bai Y, Wang K. Regulation of lncRNA and its role in cancer metastasis. Oncol Res 2016; 23: 205-217.
26) Pickl JM, Heckmann D, Ratz L, Klauck SM, Sültmann H. Novel RNA markers in prostate cancer: functional considerations and clinical translation. Biomed Res Int 2014; 2014: 765207.
27) Willard SS, Koochekpour S. Regulators of gene expression as biomarkers for prostate cancer. Am J Cancer Res 2012; 2: 620-657.
28) Xu W, Chang J, Du X, Hou J. Long non-coding RNA PCAT-1 contributes to tumorigenesis by regulating FSCN1 via miR-145-5p in prostate cancer. Biomed Pharmacother 2017; 95: 1112-1118.
29) Long Y, Wang X, Youmans DT, Cech TR. How do lncRNAs regulate transcription? Sci Adv 2017; 3: eaao2110.
30) Wang H, Huo X, Yang XR, He J, Cheng L, Wang N, Deng X, Jin H, Wang N, Wang C, Zhao F, Fang J, Yao M, Fan J, Qin W. STAT3-mediated upreg-

ulation of lncRNA HOXD-AS1 as a ceRNA facilitates liver cancer metastasis by regulating SOX4. Mol Cancer 2017; 16: 136.

31) Kurimoto K, Hayashi M, Guerrero-Preston R, Koike M, Kanda M, Hirabayashi S, Tanabe H, Takano N, Iwata N, Niwa Y, Takami H, Kobayashi D, Tanaka C, Yamada S, Nakayama G, Sugimoto H, Fujii T, Fujiwara M, Kodera Y. PAX5 gene as a novel methylation marker that predicts both clinical outcome and cisplatin sensitivity in esophageal squamous cell carcinoma. Epigenetics 2017; 12: 865-874.

32) Wu X, Xiao Y, Zhou Y, Zhou Z, Yan W. LncRNA FOXP4-AS1 is activated by PAX5 and promotes the growth of prostate cancer by sequestering miR-3184-5p to upregulate FOXP4. Cell Death Dis 2019; 10: 472.

33) Chan JJ, Tay Y. Noncoding RNA:RNA regulatory networks in cancer. Int J Mol Sci 2018; 19: 1310.

34) Kuna RS, Field SJ. GOLPH3: a Golgi phosphatidylinositol(4)phosphate effector that directs vesicle trafficking and drives cancer. J Lipid Res 2019; 60: 269-275.

35) Wu S, Fu J, Dong Y, Yi Q, Lu D, Wang W, Qi Y, Yu R, Zhou X. GOLPH3 promotes glioma progression via facilitating JAK2-STAT3 pathway activation. J Neurooncol 2018; 139: 269-279.

36) Sun J, Yang X, Zhang R, Liu S, Gan X, Xi X, Zhang Z, Feng Y, Sun Y. GOLPH3 induces epithelial-mesenchymal transition via Wnt/β-catenin signaling pathway in epithelial ovarian cancer. Cancer Med 2017; 6: 834-844.

37) Zhang Q, Zhuang J, Deng Y, Zhao X, Tang B, Yao D, Zhao W, Chang C, Lu Q, Chen W, Zhang S, Ji C, Cao L, Guo H. GOLPH3 is a potential therapeutic target and a prognostic indicator of poor survival in bladder cancer treated by cystectomy. Oncotarget 2015; 6: 32177-32192.